
FUNDAMENTALS OF

Electrospinning & Electrospun Nanofibers

Tong Lin, Ph.D.

Institute for Frontier Materials, Deakin University

Jian Fang, Ph.D.

Institute for Frontier Materials, Deakin University



DEStech Publications, Inc.

Fundamentals of Electrospinning & Electrospun Nanofibers

DEStech Publications, Inc.
439 North Duke Street
Lancaster, Pennsylvania 17602 U.S.A.

Copyright © 2017 by DEStech Publications, Inc.
All rights reserved

No part of this publication may be reproduced, stored in a retrieval system, or transmitted, in any form or by any means, electronic, mechanical, photocopying, recording, or otherwise, without the prior written permission of the publisher. The publisher is not liable for any errors resulting from the use of the CD-ROM.

Printed in the United States of America
10 9 8 7 6 5 4 3 2 1

Main entry under title:
Fundamentals of Electrospinning & Electrospun Nanofibers

A DEStech Publications book
Bibliography: p.
Includes index p. 235

Library of Congress Control Number: 2016952851
ISBN No. 978-1-60595-160-7

Contents

Foreword ix

Preface xi

1. Introduction to Nanofibers	1
1.1. Nanomaterials and Nanotechnology	1
1.2. Nanofibers	5
1.3. Nanofiber-Making Techniques	10
1.4. References	22
2. Electrospinning	25
2.1. Brief History	25
2.2. Basic Apparatus—"Needle" Based Electrospinning	30
2.3. Taylor Cone	31
2.4. Whipping and Jet Instability	32
2.5. Solution Electrospinning: Advantages and Disadvantages	34
2.6. Effect Factors of Solution Electrospinning	40
2.7. Melt-Electrospinning	52
2.8. References	54
3. Electrospun Fibers: Morphologies and Unique Properties.	67
3.1. Typical Morphology	67
3.2. Internal Structure	76
3.3. Unique Properties	77
3.4. References	78

4. Improvement of Fiber Quality	81
4.1. Main Problems	81
4.2. Improvement Methods	81
4.3. References	87
5. Advanced Needle Electrospinning	89
5.1. Second Electrode-Enhancement	89
5.2. Gas-Jacket Enhanced Electrospinning	90
5.3. Multiple Needle Electrospinning	92
5.4. Shielding Ring	92
5.5. Porous Tube Spinneret	93
5.6. Near-Field Electrospinning	94
5.7. Emulsion Electrospinning	96
5.8. Laser Induced Melt Electrospinning	98
5.9. Portable Electrospinner	99
5.10. References	102
6. Needleless Electrospinning.	105
6.1. Problems with a Single Needle Electrospinner	105
6.2. Aided by Magnetic Liquid	105
6.3. Upward Spinning	106
6.4. Downward Spinning	111
6.5. Needleless Melt Electrospinning	114
6.6. Core-Sheath Needleless Electrospinner	115
6.7. References	118
7. Control of Nanofiber Deposition	121
7.1. Fiber Alignment	121
7.2. Fibrous Tubes	124
7.3. Liquid Bath Collection	124
7.4. 3D Fibrous Structures	127
7.5. References	128
8. Nanofiber Yarns	131
8.1. Definition	131
8.2. Nanofiber Short Bundle	131
8.3. Continuous Bundles	134
8.4. Nanofiber Yarns	136
8.5. References	143

9. Applications of Electrospun Nanofibers	145
9.1. Biomedical	145
9.2. Environment	156
9.3. Electronic Devices	161
9.4. Catalysis and Enzyme	183
9.5. Other Applications	187
9.6. References	194
10. Inorganic Nanofibers	213
10.1. Carbon Nanofibers	213
10.2. Ceramic Nanofibers	214
10.3. Metal Nanofibers	217
10.4. References	219
<i>Appendix I: A Comparison of Various Solution-based Electrospinning Techniques</i>	221
<i>Appendix II. Commonly-used Characterization Methods for Electrospun Nanofibers</i>	227
<i>Index</i>	235

Foreword

IT is my pleasure to write a foreword for *Fundamentals of Electrospinning and Electrospun Nanofibers* co-authored by Tong Lin and Jian Fang. Both of the authors are experts and active researchers in their respective fields. Professor Lin and his team, including Dr. Fang, are well-known for their innovative research in nanofiber science and engineering with numerous contributions in the forms of many high-quality original publications and patented electrospinning technologies for large-scale nanofiber production and continuous nanoyarn spinning.

In this book, the authors provide the fundamental science to understand the scientific basis of electrospinning, and then extend the basic knowledge to the technology development, covering almost all aspects of electrospinning and electrospun nanofibers, including the history of electrospinning, the nanofiber electrospinning mechanism, the importance of nanofibrous materials and structure control, the formation of multicomponent nanofibers, the two-dimensional nanofiber nonwovens, the advanced three-dimensional nanofibrous structures and continuous nanofiber yarns, and the functional applications of electrospun nanofibers and nanofiber yarns in diverse systems.

The above approach should enable students to systematically gain insight into the field while experienced academic and industrial professionals can use this book to quickly review this challenging multidisciplinary field for the latest developments, to broaden their knowledge of electrospinning, and to develop practical systems. Therefore, this book will be useful to both students who are merely curious about the possibilities that electrospinning can offer and those researchers who

actively work in materials science and engineering, nanotechnology, fibers and textiles, and other related areas. I am confident that it will be a valuable resource to promote the development of various electrospun nanofibers and yarns for practical applications.

LIMING DAI
Kent Hale Smith Professor
Case Western Reserve University, USA
June 2016

Preface

ELECTROSPINNING, previously also known as “electrostatic spinning,” was discovered a century ago, and it has become a popular technique to prepare nanofibers. Recent decades have seen a number of innovative developments in relation to both electrospinning and electrospun nanofiber. Many unique properties of electrospun nanofibers have been uncovered, making electrospinning distinctive from other nanofiber making methods. These research developments have greatly enriched our understanding on such a one-dimensional material and the technical principle. They offered technological solutions to obtain nanofibers of diverse morphologies, fibrous structures, and compositions for various research purposes.

We are very pleased to note that electrospun nanofibers have already been used in some practical niches. The development of needleless electrospinning has allowed the mass production of nanofibers. Tens of thousands of researchers have been involved in electrospinning related works, and the number of researchers grows increasingly with more and more applications of electrospun nanofibers in practice.

The purpose of this book is to provide a systematic introduction of electrospinning and electrospun nanofibers. It is written based on Professor Tong Lin’s syllabus to teach the nanotechnology majored students at Deakin University, Australia, and postgraduate students who attended the 2013 Donghua University Summer Courses in Shanghai, China. His lectures received enthusiastic responses, which formed one of the motivations to write this book. We hope the book can be used as a textbook for the undergraduate and postgraduate students who study

the fibers or materials-related subjects to broaden their professional knowledge.

The book also covers key research results on electrospinning and electrospun nanofibers published in literature through 2015. It also helps people from different backgrounds to rapidly understand this fiber-making technology and the interesting fibers.

The book consists of 10 chapters. Chapter 1 provides introductory information on the importance of nanofibers, their uniqueness, naturally occurring nanofibers, and all the nanofiber making techniques developed. Chapter 2 introduces history and fundamentals of electrospinning, fiber forming, and major parameters affecting the electrospinning process. Chapter 3 deals with the typical morphology and structure of electrospun nanofibers. Chapter 4 discusses main problems existing in electrospinning nanofibers and the approaches to improving fiber quality. Chapter 5 reviews various developments on needle-based electrospinning. Chapter 6 describes the development of needleless electrospinning for large scale nanofiber production. Chapter 7 details the approaches to controlling fiber deposition for making structured nanofibrous assemblies. Chapter 8 is about nanofiber yarns and their properties. Chapters 9 summarizes the applications of electrospun nanofibers in various fields. Chapter 10 introduces methods to prepare carbon, inorganic, and metal nanofibers based on electrospinning.

Due to the rapid progress in the electrospinning field and the limited time for the authors to write the book, some omissions may have occurred. We do apologize about this, and, if the reader finds any omissions, we would appreciate it if you could let the authors know. We promise we will add them to the later edition.

Electrospinning

2.1. BRIEF HISTORY

2.1.1. Electrostatic Phenomenon

THE principle of electrospinning is the phenomenon of electrostatic attraction which was discovered more than 400 years ago. In 1600, Englishman William Gilbert found that when a piece of rubbed amber was held close to a water drop, the droplet could be drawn toward the amber and form a cone shape [1]. It is known that “like charges repel and dislike charges attract.” It is the electrostatic attraction between opposite charges that causes water droplet deformation, and the force involved follows the Coulomb’s law:

$$F = \frac{k \cdot Q_1 \cdot Q_2}{d^2} \quad (2.1)$$

where Q_1 and Q_2 represent the charges on the two objects (in Coulombs, C), d is the distance between the charges objects (in meters, m), and k is the Coulomb’s law constant, approximately $9.0 \times 10^9 \text{ N}\cdot\text{m}^2/\text{C}^2$.

2.1.2. Electropray

After Gilbert’s observation of electrostatic force, French physicist Jean-Antoine Nollet experimentally investigated the behavior of water through an electrified capillary. He found that an intermittent water dripping from the capillary was turned to a continuous spraying once

the water was electrified [2]. After careful examination on the capillary material, capillary size, liquid type, and flow format, Nollet concluded that electricity speeded up the liquid flow when it came out of the capillary drop-by-drop under gravity, and the flow was accelerated with a narrower capillary. However, he did not find the same effect of acceleration when the liquid flowed out of the capillary in a continuous format.

John Zeleny conducted a detailed study on this spraying phenomenon and discussed the scientific principles in his papers published in 1914 [3] and 1917 [4]. In the first study, Zeleny used a pointed conductor to investigate the effect of electricity polarity, electric potential, conductor size, and liquid temperature on spraying and the formation of liquid meniscus at the conductor. In his later experiment, a glass tube with an inner diameter of 0.92 mm was used as capillary. Ethyl alcohol was loaded into the tube and charged to several thousand volts for spraying. A grounded plate was placed 2 cm away from the collector. A series of images of the droplet at the tube tip were taken during the spraying process. For the first time in history, time-lapse images of liquid meniscus were recorded. By changing the applied voltage and hydrostatic pressure in the tube, different spray behaviors were observed, such as straight stream, bended stream, stream splitting, and clouding after straight stream. Early development in electro spray has found its application in surface painting, however it was not until the later work done by Geoffrey Taylor that electro spray was applied widely in many other areas. In this theoretical study [5], Taylor modelled the formation of cone-shaped liquid protrusion by the influence of an electric field. He concluded that a semi-angle conical angle of 49.3° should be obtained at a stable air-fluid interface, and this cone structure formed during electro spray, and also in electro spinning, which was named the "Taylor cone," after him.

Today, electro spray has been the main ionization source in mass spectrometry for chemical and biochemical analysis, and it is also known as "electro spray ionization." In a typical process illustrated in Figure 2.1, a solution containing analyte molecules is loaded into a spraying nozzle, which is charged by a power source. Once a high voltage is applied by the power source, the solution is drawn out of the capillary nozzle. With increasing the applied voltage, a Taylor cone is formed toward the counter electrode. When the electrostatic force is high enough to overcome solution surface tension, a fine solution jet containing many solution droplets is ejected from the cone apex. With the evaporation of the solvent in the solution, the droplets shrink in

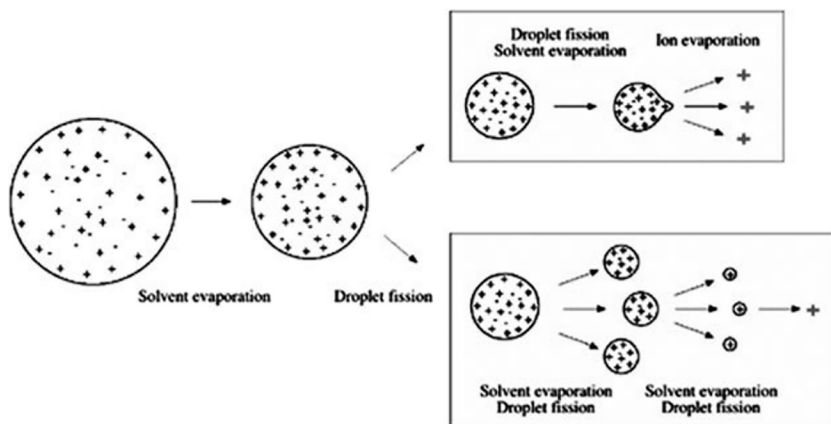


FIGURE 2.1. Electro spray ionization process [7].

size and eventually reach the limit where their surface tension is not able to sustain the electrostatic repulsion force among the charges carried. A Coulomb explosion then happens to break the droplet into many smaller particles and this leads to the formation of analyte ions. Two different ion formation mechanisms have been proposed: ion evaporation theory and charge residue theory [6]. In the first model, solvated ions can be directly emitted from the charged particles once the particle size is small enough to generate a high local electric field. The second model relies on the complete evaporation of solvent to form analyte ions. Other important application fields of electrospray include nanoparticle fabrication, surface functionalization, drug encapsulation, ink-jet printing, and air purification.

2.1.3. Early Techniques and Development

From Gilbert's observation in the seventeenth to the nineteenth century, the advancement of science and technology has greatly improved the understanding on many naturally occurring phenomena and has contributed to a large number of inventions in machinery and processing. Due to the high price of natural fiber products (such as silk and wool fabrics), ongoing efforts have been made since the nineteenth century to produce artificial fiber as the alternative. Started from the materials like glass, nitrocellulose, and collodion, an enormous number of materials have been investigated and it was not until 1920s that the first artificial fiber, Rayon, was fully commercialized.

During the study on artificial fibers, many scientists have introduced electrostatic charge or electric field in their setups. However, due to the difficulty either in scaling up the fiber production or finding proper instruments to observe the fiber morphology, none of their efforts have directly resulted in a significant advancement in electric field assisted fiber spinning.

In 1900, a patent filed in the United Kingdom by John F. Cooley has been considered as the first patent on electrospinning [8]. As shown in Figure 2.2(a), The Cooley setup had a glass tube with one capillary end. One bulb was used for delivering the spinning solution downward. Two electrodes from an electric-current generator were placed close to the tube capillary. Fibers were electrostatically generated from the tube due to the electric field difference between the electrodes. The produced fibers were collected by a reel. In his invention, Cooley proposed several different types of tubes as the spinneret. The basic tube [Figure 2.2(b)] had a core-sheath structure with an inner tube for delivery of spinning solution and an outer tube for carrying supplementary liquid or solvent. In a modified tube shown in Figure 2.2(c), a spraying tube was fitted to the basic tube for carrying steam jet or compressed air. Further modification reduced the basic tube length and changed the capillary end of the tube to a wider open exit. The spinning solution delivered through the basic tube was transferred to a second tube with a funnel-like end. By rotating the second tube, fiber spinning could be conducted from the edge of the funnel, as shown in Figure 2.2(d).

Almost at the same time, William J. Morton filed his patent on using an electrical method to disperse fluid [9]. His setup applied electrodes either outside or inside the spinning solution to produce fiber web or thread. A collecting reel was also used to wind up the prepared thread.

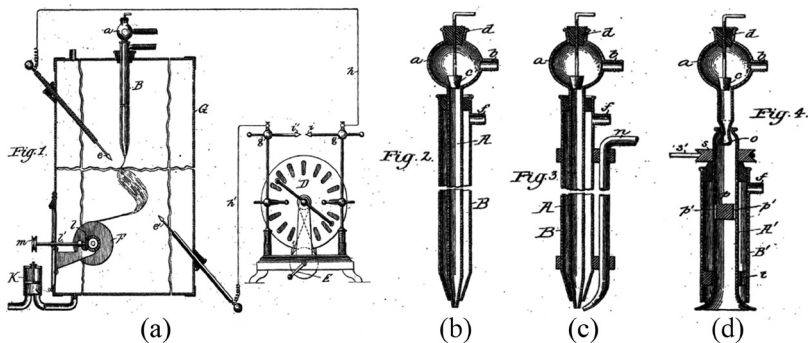


FIGURE 2.2. Illustrated setup in the first electrospinning setup [8].

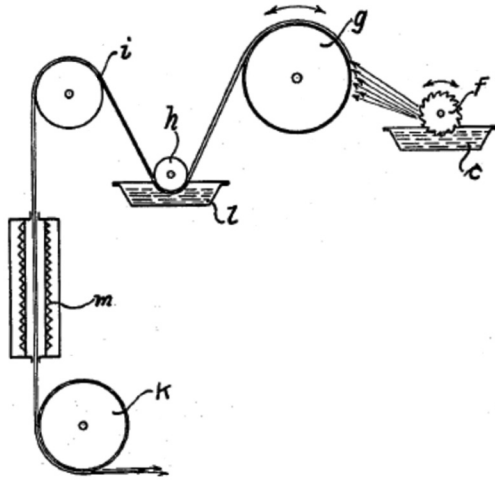


FIGURE 2.3. Illustrated setup in an early patent by Formhals [10].

Another great contributor to electrospinning is Anton Formhals who filed a series of patents on electrospinning setups between 1931 and 1944 [10–12]. In one of this patents [10], Formhals proposed the idea of commercial benefit to produce continuous fiber threads with the assistance of an electric field. Figure 2.3 shows the basic setup in the patent. An electric field was generated between the serrated wheel [Figure 2.3(f)] and the metal ring [Figure 2.3(g)]. By rotating the wheel and the ring in the same or opposite directions, the spinning solution was carried out of the vessel [Figure 2.3(c)] by the wheel. Fine fibers were generated from the wheel and they were collected by the ring. The design even contained a washing device [Figures 2.3(h) and 2.3(i)] and a heating component [Figure 2.3(m)] for continuous production.

After Formhals' patents in the 1930s, the most significant advance in the field of electrospinning was the contribution by Geoffrey Taylor to theoretically understand the droplet deformation under an electric field and the mathematical explanation of the “Taylor cone.” Then in the early 1990s, Dr. Darrell H. Reneker from The University of Arkon re-examined the effect of electrostatic force on fiber formation from a polymeric solution [13]. Thanks to the emerging of nanotechnology, Reneker's work immediately drew an enormous interest from both academia and industry, and the terms “electrospinning” and “nanofibers” have been popularized ever since.

It was not until the publication of a book [14] that the great advancement in electrospinning made by scientists in the former Soviet Union

has become clear to us. From the late 1930s [15], Nathalie D. Rozenblum and Igor V. Petryanov-Sokolov from the Aerosol Laboratory in the L. Ya Karpov Institute started production of electrospun nanofibers. They used cellulose acetate to produce nanofiber webs for air filtration, and the filters are now known as “Petryanov filters.” Due to the military application of their face masks in filtering radioactive particles, the work has been kept as a secret for decades. However, the achievement made at that time was significant. The first factory for producing nanofibers was built in 1939, and the productivity of nanofiber based filtration materials reached 20 million square meters per year by the 1960s.

2.2. BASIC APPARATUS—“NEEDLE” BASED ELECTROSPINNING

The basic setup for electrospinning can be very simple. As shown in Figure 2.4, a typical needle-based electrospinning setup consists of a syringe as the container for carrying polymer solution or melt, a high voltage power supply, a metal needle as a spinneret, and a grounded collector. During electrospinning of a polymer solution, the solution is delivered to the nozzle tip. The accumulation of solution will form a droplet at the needle tip and fall off under the gravity if there is no interaction of an electric field. However once a high voltage is applied to the polymer solution, an electric field difference is formed between the solution and the collector. This difference can deform the solution droplet and form a Taylor cone. With the increase in the applied voltage, a solution jet is ejected from the Taylor cone immediately after the electrostatic force exceeds the surface tension of the polymer solution. After this initial stage, the stable jet becomes unstable and it undergoes a bending (or whipping) movement caused mainly by columbic

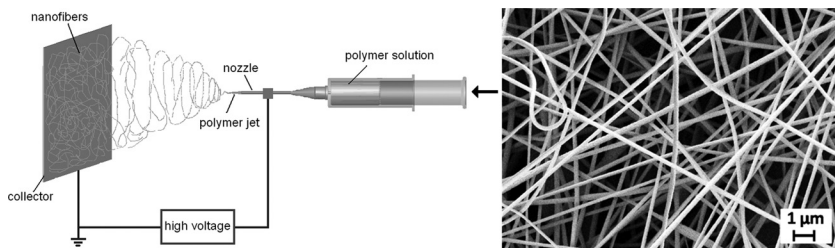


FIGURE 2.4. Typical needle based electrospinning setup and SEM image of electrospun nanofibers [16].

repulsion, which stretches the jet into fine fibers. With the evaporation of solvent from the filaments, dry or semidry nanofibers are formed and deposited on the collector. Normally, electrospun nanofibers have a random fiber orientation on the collector (Figure 2.4), and an interconnected porous structure can be formed on the nanofiber webs.

2.3. TAYLOR CONE

The Taylor cone was intensively investigated by Geoffrey Taylor during his research work on electrospray. However it is also important in the process of electrospinning (Figure 2.5). In Taylor's theory [5], a solution droplet tends to deform its shape into a conical structure once it is subject to an electric field with a certain intensity. Increasing the applied voltage enhances the electrostatic repulsion force among the charges in the cone, and once the charges density reaches the limit (Rayleigh limit), a solution jet will be ejected from cone tip. As mentioned, a perfect cone should have a full angle of 98.6° and is formed right before the jet initiation.

However due to the high viscosity of the spinning solution, a Taylor cone tends to have different angles in electrospinning. Yarin *et al.* [18] developed a mathematic model to calculate a Taylor cone. His work suggested that a Taylor cone can only be formed from self-similar solutions, and a smaller cone angle is usually generated from nonself-similar solutions. When a 6% polyethylene oxide (PEO, Mw 400,000) solution

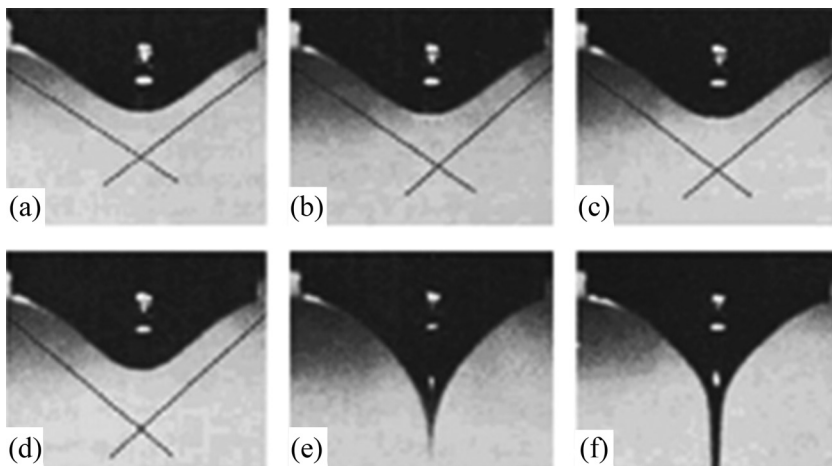


FIGURE 2.5. Evolution of Taylor cone during electrospinning [17].

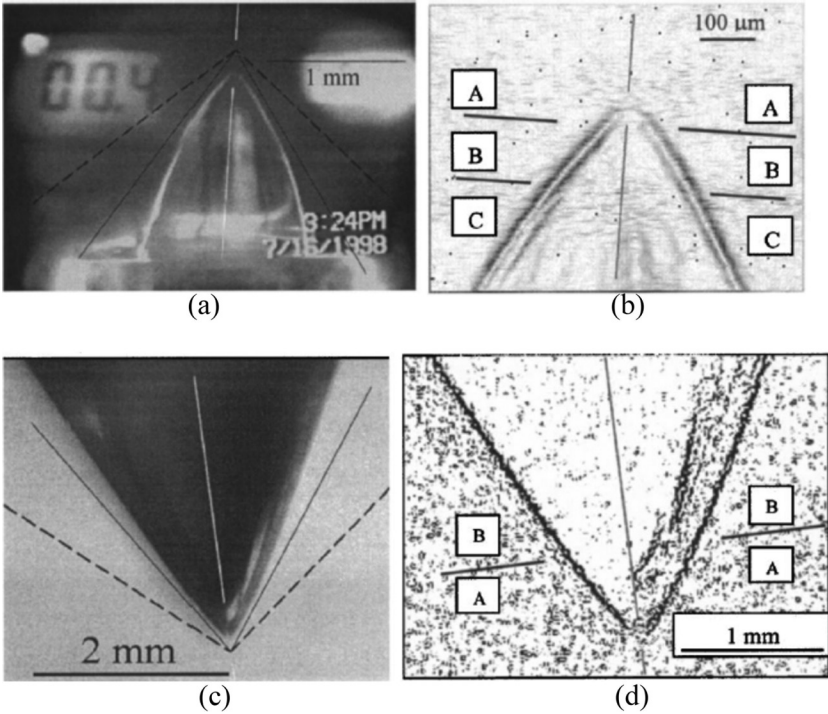


FIGURE 2.6. Digital photos: (a) and (c) and processed images; (b) and (d) of Taylor cone in upward and downward electrospinning processes [18].

is electrospun in a upward or a downward configuration (Figure 2.6), a half cone angle of 33.5° is formed in the upward electrospinning, while the angle for the downward electrospinning is 31° .

2.4. WHIPPING AND JET INSTABILITY

Fiber stretching during an electrospinning process can be divided into three stages: jet initiation, whipping (or bending) instability, and fiber deposition [19]. From the initial jet to dry fibers, electrospinning takes place very rapidly, typically in milliseconds [20,21].

The threshold voltage required to initiate solution jet in an electrospinning process can be mathematically described using the Equation (2.2):

$$V_c^2 = 4 \frac{H^2}{L^2} \left(\ln \frac{2L}{R} - \frac{3}{2} \right) (0.0117\pi R\gamma) \tag{2.2}$$

where H is the spinning distance, L is the length of the capillary spinneret, R is the capillary radius, and γ is the solution surface tension.

When the electrospinning process is observed by normal cameras, the long exposure time limits their revealing the jet behavior. As seen in Figure 2.7(a), the solution jet appears to be split into many smaller jets. The early theory of fiber thinning in electrospinning was considered as the repeated jet splitting. Later observations on the electrospinning process using high speed video cameras [20] indicated that the jet followed a bending, winding, spiraling, and looping path after the initial stable stage [Figure 2.7(b)]. The jet became longer and thinner during this instability process. The bending instability has been described by theoretical models [18,20,23–25]. As described by Reneker and Yarin [20,23], a viscoelastic model for the electrified jet was developed and the net normal force, F , acting on a jet element was given by Equation (2.3):

$$dF = |k| d\zeta \left[\pi a \sigma - e^2 \ln \frac{L}{a} \right] \quad (2.3)$$

where k is the jet curvature, ζ is co-ordinate system along the central axis of the bend jet, a is the jet cross-section radius, σ is the surface tension coefficient, e is the charge density, and L represents the jet length scale.

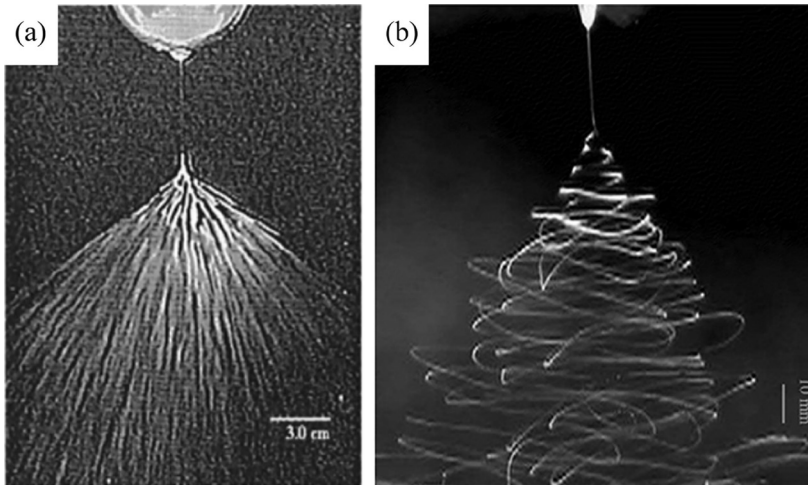


FIGURE 2.7. Images of an electrospinning process taken by (a) a normal camera [20] and (b) a high speed camera [22].

The momentless quasi-1D equation was given using a Lagrangian parameter “frozen” into the jet elements:

$$\lambda f = \lambda_0 f_0 \quad (2.4)$$

$$\rho \lambda_0 f_0 \frac{\partial V}{\partial t} = \tau \frac{\partial P}{\partial s} + \lambda |k| P n - \rho g \lambda_0 f_0 k + \lambda |k| \left(\pi a \sigma - q_{el} \ln \frac{L}{a} \right) n - \lambda e \frac{U_0}{h} k \quad (2.5)$$

Equation (2.4) is the continuity equation with λ being the geometrical stretching ratio, so that, $\lambda ds = d\xi$ and $f = \pi \alpha^2$ the cross-sectional area. Subscript zero denotes the parameter values at time $t = 0$. Equation (2.5) is the momentum balance equation in which λ represents the geometrical stretching ratio, $f = \pi \alpha^2$ is the cross-sectional area, ρ is the liquid density, V is velocity vector, P is the longitudinal force in the jet cross-section, U_0/h is the outer electric field strength, and q_{el} is the net coulomb force acting on a jet element from all the other elements depending on e and the current overall configuration of the jet. The right-hand side of Equation (2.5) includes the longitudinal internal force of rheological origin acting on the jet (the first two terms), the gravity force (the third term), the bending electrical force and the stabilizing effect of the surface tension (the fourth term), and the electrical force acting on the jet from electric field created by the potential difference of the starting point of the jet and the collector.

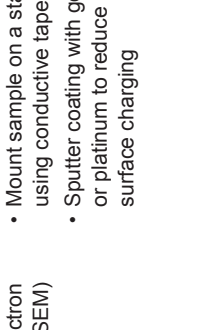
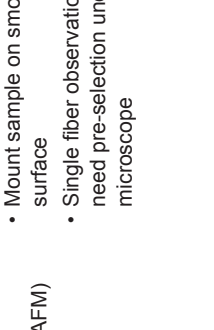
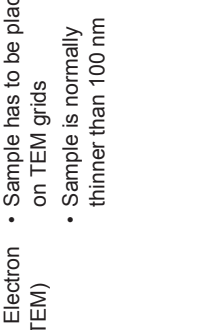
2.5. SOLUTION ELECTROSPINNING: ADVANTAGES AND DISADVANTAGES

Electrospinning of nanofibers requires a viscous semiconductive fluid to initiate fluid jet and maintain a fibrous structure during jet stretching, bending, and thinning. The most common fluid used for electrospinning is a polymer solution. The majority of research on electrospinning and electrospun nanofibers have been conducted based on a solution-based spinning process, which possesses many advantages.

2.5.1. Advantages

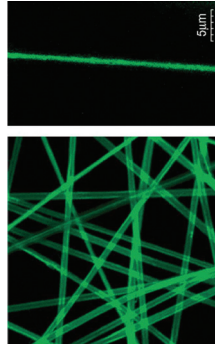
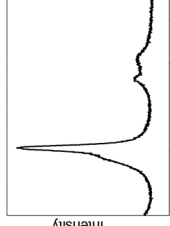
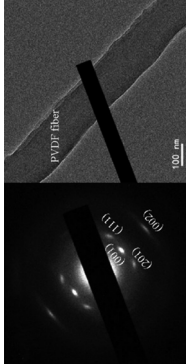
A variety of polymers could be used for making an electrospinning solution, and this allows to produce nanofibers from a wide range of polymer materials, either natural or synthetic. In most cases, polymers suitable for processing into nanofibers through electrospinning have a

APPENDIX II. Commonly-used Characterization Methods for Electrospun Nanofibers.

Methods	Sample Preparation	Information	Typical Examples
Scanning Electron Microscopy (SEM)	<ul style="list-style-type: none"> Mount sample on a stage using conductive tape Sputter coating with gold or platinum to reduce surface charging 	<ul style="list-style-type: none"> Surface morphology and fiber alignment Based on SEM images, fiber diameter, diameter distribution, degree of fiber alignment, can be calculated using image processing software 	
Atomic Force Microscopy (AFM)	<ul style="list-style-type: none"> Mount sample on smooth surface Single fiber observation need pre-selection under microscope 	<ul style="list-style-type: none"> Direct observation of fiber surface morphology and alignment Surface roughness High profile Mechanical properties of single nanofibers 	
Transmission Electron Microscopy (TEM)	<ul style="list-style-type: none"> Sample has to be placed on TEM grids Sample is normally thinner than 100 nm 	<ul style="list-style-type: none"> Direct observation of fiber surface morphology Transmission of electron beam shows materials encapsulated within the fibers, core-sheath or hollow structure 	

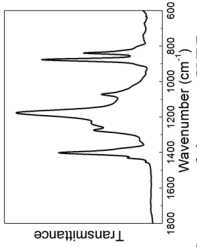
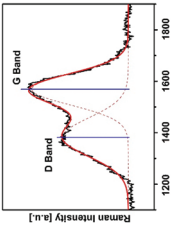
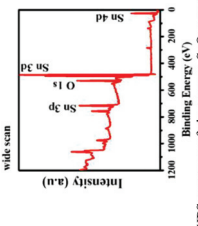
(continued)

APPENDIX II (continued). Commonly-used Characterization Methods for Electrospun Nanofibers.

Methods	Sample Preparation	Information	Typical Examples
Confocal Microscopy	<ul style="list-style-type: none"> • A fluorescent indicator is often added into polymer solution for making nanofibers 	<ul style="list-style-type: none"> • Observation of fiber surface morphology and alignment • Observation of three-dimensional morphology of a fibrous structure • Test porosity and pore size of a fibrous matrix 	
X-ray diffraction (XRD)	<ul style="list-style-type: none"> • Mounting fiber bundle or fiber sheet on the instrument stage 	<ul style="list-style-type: none"> • Crystal structure • Crystal phase • Preferred orientation • Inter-plane spacing • Crystal size 	 <p data-bbox="691 263 709 558">XRD curve of electrospun PVDF nanofibers</p>
Selected area electron diffraction (SAED) (normally equipped in TEM)	<ul style="list-style-type: none"> • Same as TEM sample preparation 	<ul style="list-style-type: none"> • Crystal structure • Crystal phase • Macromolecular chain orientation 	 <p data-bbox="916 246 932 576">SAED pattern of single PVDF nanofiber</p>

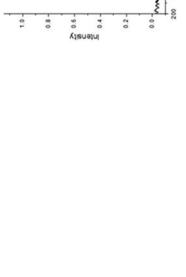
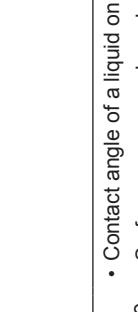
(continued)

APPENDIX II (continued). Commonly-used Characterization Methods for Electrospun Nanofibers.

Methods	Sample Preparation	Information	Typical Examples
Fourier Transform Infrared spectrum (FTIR)	<ul style="list-style-type: none"> Reflection mode: a fiber bundle or a fiber sheet is placed on the sample stage in the instrument Transmission mode: chopped fibers are mixed with KBr and pressed into a pellet 	<ul style="list-style-type: none"> Chemical bond vibration Crystal phase feature and calculation of crystal phase content Polarized FTIR can measure bond orientation within sample 	 <p>FTIR spectrum of electrospun PVDF nanofibers</p>
Raman spectroscopy	<ul style="list-style-type: none"> A fiber bundle or a fiber sheet is mounted on the sample holder 	<ul style="list-style-type: none"> Symmetric chemical bond vibrations Crystal orientation 	 <p>Typical Raman spectrum with D band and G band</p>
X-ray photoelectron spectroscopy (XPS)	<ul style="list-style-type: none"> Fiber sample is mounted on sample stage in the instrument 	<ul style="list-style-type: none"> Sample surface element Chemical state Electronic state Binding energy 	 <p>XPS spectrum of electrospun SnO₂ nanofibers</p>

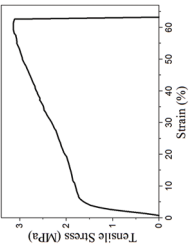
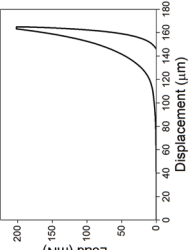
(continued)

APPENDIX II (continued). Commonly-used Characterization Methods for Electrospun Nanofibers.

Methods	Sample Preparation	Information	Typical Examples
Solid nuclear magnetic resonance (NMR)	<ul style="list-style-type: none"> A fiber sample is loaded into a NMR tube for NMR testing 	<ul style="list-style-type: none"> Chemical structure Materials purity Molecular conformation 	 <p style="text-align: center;">Solid NMR spectrum of electrospun PVA nanofibers</p>
Contact angle (CA)	<ul style="list-style-type: none"> Placing fibrous mat sample on sample stage 	<ul style="list-style-type: none"> Contact angle of a liquid on a nanofiber web Surface energy can be calculated based on CA result 	
Mercury porosimetry	<ul style="list-style-type: none"> Fibrous sample with sufficient thickness 	<ul style="list-style-type: none"> Porosity of electrospun nanofiber web of different conditions (porosity can also be estimated based on material density and web density) Pore size distribution 	
Air permeability	<ul style="list-style-type: none"> Placing a fibrous sheet sample with the required shape and size on the sample holder 	<ul style="list-style-type: none"> Air permeability 	

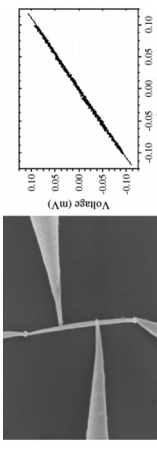
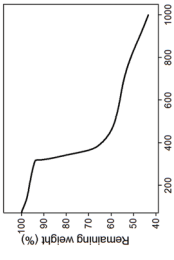
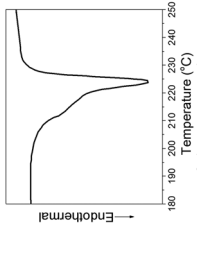
(continued)

APPENDIX II (continued). Commonly-used Characterization Methods for Electrospun Nanofibers.

Methods	Sample Preparation	Information	Typical Examples
Particles penetration rate	<ul style="list-style-type: none"> Placing a fibrous sheet sample with the required shape and size on the sample holder 	<ul style="list-style-type: none"> Particle filtration efficiency and pressure resistance Filter loading capacity 	
Tensile testing	<ul style="list-style-type: none"> Fibrous mat: cutting fibrous mat into the required shape and dimension, and the sample is then fixed on the tester Nanofiber yarn: directly fix the yarn sample on the tensile tester Single nanofiber: Collecting single using a paper or plastic frame; mounting the fiber loaded frame on the test; and then cut off the two edges of the frame. (Single nanofiber can also be tested on AFM) 	<ul style="list-style-type: none"> Tensile strength Elongation at break Modulus Toughness 	 <p>Stress-strain curve of electrospun PEU/PAN composite nanofiber web</p>
Compression testing	<ul style="list-style-type: none"> Single nanofiber: compression property can be tested on AFM Nanofiber web: fibrous mat with sufficient thickness. 	<ul style="list-style-type: none"> Load-displacement relationship Compressive modulus Nanofiber web structure stability 	 <p>Load-displacement curve of electrospun PVDF nanofiber web</p>

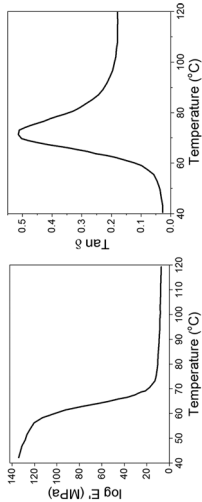
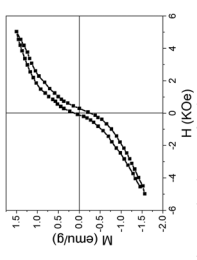
(continued)

APPENDIX II (continued). Commonly-used Characterization Methods for Electrospun Nanofibers.

Methods	Sample Preparation	Information	Typical Examples
<p>Electrical conductivity (two-probe, and four probe testing methods)</p>	<ul style="list-style-type: none"> Two probe method: to test resistance of nanofiber web, nanofiber bundle or single nanofiber. Four-probe method: mounting the sample on four probe electrodes 	<ul style="list-style-type: none"> Electrical conductivity (two-probe, and four probe testing methods) 	 <p>A four-probe electrical conductivity measurement on a single gold nanowire revealed its linear response of voltage to applied current.</p>
<p>Thermogravimetric analysis (TGA)</p>	<ul style="list-style-type: none"> Load a small amount of nanofibers into a crucible pan 	<ul style="list-style-type: none"> Weight change with temperature Moisture content Evaporation rate as a function of temperature Determination of Curie temperature Determination of materials purity Thermal degradation Thermal oxidation Material composition in blend or composite 	 <p>TGA curve of electrospun PAN nanofibers</p>
<p>Differential scanning calorimetry (DSC)</p>	<ul style="list-style-type: none"> Same as TGA 	<ul style="list-style-type: none"> Melting temperature Glass transition temperature Enthalpy of transition Crystallinity Crystallization temperature 	 <p>DSC curve of electrospun Nylon 6 nanofibers</p>

(continued)

APPENDIX II (continued). Commonly-used Characterization Methods for Electrospun Nanofibers.

Methods	Sample Preparation	Information	Typical Examples
Dynamic mechanical analysis (DMA)	<ul style="list-style-type: none"> A piece of nanofiber web is mounted with fixed into DMA chamber using two grips in tensile mode Multiple layers of nanofiber web is placed between two plates in DMA for compression mode 	<ul style="list-style-type: none"> Glass transition temperature Elastic, storage and loss modulus Loss factor Stiffness 	 <p>DMA results of electrospun PLLA nanofibers</p>
Magnetic property	<ul style="list-style-type: none"> Magnetic materials are prepared into nanofibrous structure Magnetic nanomaterials can also be added into hosting nanofibers A piece of magnetic nanofiber web is tested on magnetometer 	<ul style="list-style-type: none"> Magnetic hysteresis loop of the magnetic nanofibers in an alternating gradient magnetic field at various temperatures Magnetization curves 	 <p>Magnetic hysteresis loop of electrospun α-Fe₂O₃ nanofibers calculated at 600 °C</p>

Index

- aa0, 13, 14
- additives, 35, 154
- aerosol, 30, 157, 201
- air-jacket, 90, 91
- aligned, 17, 44, 77, 90, 116, 121–124, 132, 133, 135, 138, 149, 150–152, 161, 168, 170, 176, 179, 187
- alignment, 76, 77, 81, 121, 123, 128, 130, 136, 138, 143, 149–151, 184, 187, 197, 198, 208, 214, 228, 229
- anisotropic, 22, 57, 121, 130
- annealing, 76, 99, 217
- anode, 78, 161, 162, 163, 164, 202, 205
- antibacterial, 62, 153, 154, 199, 204
- assembly, 9, 22, 23, 55, 56, 78, 118, 133, 136, 208
- attachment, 122, 146–150, 153
- auxiliary electrode, 92

- battery, 39, 63, 161–164, 202
- beads, 40, 42, 44, 64, 81, 82, 86, 88
- beads-free, 82
- beads-on-string, 40–42
- bi-component, 12, 19, 70, 73, 74, 116, 165
- biocompatibility, 186, 187, 197
- biomaterial, 84
- biosensors, 36, 37, 55, 207
- bubble-electrospinning, 118

- calcination, 73, 171, 175, 213, 215, 217
- capacitance, 164–167, 193, 202, 204, 214
- capacitor, 39, 170
- carbon nanofiber, 56, 57, 193, 206
- carbonization, 164, 165, 193, 213, 214
- catalyst, 20, 78, 173, 183, 184, 186
- cathode, 78, 161–164, 203
- centrifugal, 18, 23
- ceramic, 35, 56, 64, 73, 79, 130, 208, 209, 213–217
- co-electrospinning, 70, 73, 79
- coaxial-electrospinning, 150
- colloid, 61, 209
- core-sheath, 17, 28, 57, 67, 70, 72, 73, 96, 98, 103, 115–119, 150, 156, 162, 164, 176, 222, 224, 226, 228
- corona, 45, 105, 112
- crosslinking, 81, 84, 158, 179, 186, 187

- diameter, 7–10, 12, 13, 15, 17, 18, 21, 26, 36–39, 42, 44, 46, 48–53, 62, 65, 74, 77, 78, 82, 83, 86, 93, 94, 96, 99, 106–112, 114–116, 122, 124, 131, 133, 134, 138, 140, 142, 143, 146, 147, 149, 151, 154, 157, 181, 184, 194, 195, 197, 198, 208, 213–215, 217, 223, 225, 226, 228
- direct-current, 44

- direct-write, 89, 94, 205
 dry-drawing, 144, 211
- elastomeric, 74, 79, 84, 194, 196
 electrochemical, 54, 58, 164, 165, 173, 193, 202–206, 211
 electrode, 26, 49, 50, 65, 73, 90, 92, 93, 100, 102, 116, 121–123, 128, 132, 136, 162–164, 166, 168, 171–174, 202–204, 208, 217, 219, 222
 electrode-enhancement, 89
 electrospinner, 99, 105, 115, 138, 139
 electrospinning, 10, 17, 18, 23, 25, 26, 28–40, 42–46, 48–74, 76, 78, 79, 81, 82, 84, 86, 88–96, 98–103, 105–119, 121–124, 127, 128, 130–137, 143–145, 150, 153–156, 161, 162, 164, 167, 168, 170, 174, 179, 181, 183, 184, 186, 187, 194–200, 202–204, 207–211, 213–215, 217, 219, 221–226
 electrospray, 25–27, 31, 40, 54
 electrostatic, 15, 17, 25–31, 41, 46, 48, 50, 55, 59, 67, 69, 89, 94, 118, 130, 164, 199
 emulsion, 35, 96, 102, 103, 116, 119, 159, 224
 entanglement, 41, 42, 81, 124
 enzyme, 155, 156, 176, 183, 185, 186, 200, 209, 210
- fabrication, 27, 54, 55, 57, 59–61, 63, 64, 79, 119, 128, 130, 143, 144, 179, 180, 191, 196, 197, 201, 202, 204, 206, 208–210, 219
 fabrics, 7, 23, 27, 61, 130, 157, 158, 161, 170, 191, 194, 202
 filler, 81, 86, 133
 filter, 9, 157–159, 201, 232
 fingerprint, 189, 190
 forspinning, 23
- gas-jacket, 90, 91, 223
- hard-templating, 10, 13, 14
 hierarchical, 22, 147, 186, 216, 219
 high-voltage, 100
- hollow, 8, 17, 64, 67, 72, 73, 79, 102, 116, 134, 167, 204, 222, 224, 226, 228
 hybrid, 35, 60, 130, 143, 144, 168, 191, 192, 205, 211, 219
- immiscible, 96, 115, 118, 159
 inter-electrode, 183
 inter-fiber, 9, 124, 135, 151, 164, 165, 217
 islands-in-the-sea, 12
- jet-whipping, 82
- knitted, 191
- laser-electrospinning, 99, 103
 lithium-ion batteries, 161
- macromolecular, 55, 57, 59, 60, 63, 65, 76, 78, 103, 143, 144, 200, 202, 205, 206, 209, 210, 229
 magnetospinning, 10, 12
 melt-blown, 10, 13
 melt-electrospinning, 52, 53, 65, 99, 100, 103
 microfiber, 61, 148, 149, 151, 195
 modification, 28, 138, 147, 161, 184
 moisture, 42, 50, 51, 69, 152, 154, 215, 233
 multi-component, 216
- nanofiber, 7, 9, 10, 11, 15–17, 19, 20, 22–24, 30, 31, 43, 48, 49, 55–63, 65, 67, 70, 73, 77–79, 83–87, 92–94, 102, 105, 106, 113, 121, 123, 124, 127, 128, 131–140, 142–162, 164, 166–168, 170, 172–174, 176, 179–181, 183, 184, 186–198, 200–209, 211, 213, 214, 217, 219, 224, 231–234
 nanomaterial, 156
 nanoparticle, 27, 173, 184, 202
 nanostructured, 60, 200, 206, 219
 nanotube, 88, 166, 174, 193, 201, 214
 nanowire, 168, 183, 205, 206
 needle-based, 30
 nonwoven, 17, 23, 157–159, 161, 168, 202

- orientation, 19, 31, 52, 57, 78, 90, 102–122, 124, 128, 130, 132, 133, 138, 149, 150, 151, 194, 222, 229, 230
- porosity, 78, 143, 145, 147, 153, 155, 159, 161, 162, 194, 229, 231
- portable, 89, 99, 100, 103, 190, 224
- pseudocapacitor, 164, 166

- randomly oriented, 13, 17

- scaffold, 36, 39, 56–58, 60–62, 127, 130, 145–152, 159, 191–195, 197, 200, 201, 207, 211
- self-assembly, 10, 15, 16
- self-crimping, 79
- semi-conducting, 134
- semiconductor, 171, 176, 183, 207
- sensor, 36, 56, 78, 168, 175, 176, 205, 213
- separator, 78, 162, 164, 166, 202
- soft-templating, 10, 14
- solidification, 7, 16, 45, 51, 90
- solvent, 12, 21, 26–28, 31, 35–43, 45, 46, 50–52, 57, 61, 64, 67–71, 74, 76, 79, 84, 86, 90, 91, 116, 118, 124, 136, 156, 172, 225, 226

- sound absorption, 61, 160
- spinnability, 42, 43, 84, 215
- spinneret, 12, 28, 30, 33, 70, 73, 74, 90–94, 99, 102, 105–111, 113–116, 118, 226
- supercapacitor, 78, 161, 164, 166, 167, 193, 203–205, 214
- syringe, 30, 45, 96, 102

- temperature, 10, 16, 20, 21, 26, 35, 40, 51–53, 61, 70, 76, 99, 114, 115, 165, 167, 173, 184, 207, 213, 215, 233, 234
- three-dimensional, 130, 196, 197, 206, 229
- tissue-engineering, 130
- twist, 132, 133, 136–138, 140, 142, 143

- viscoelastic, 33, 40, 41, 60
- voltage, 17, 19, 26, 30–32, 40, 43–46, 49–51, 57, 89–91, 94, 96, 100, 105–116, 132, 155, 163, 168, 170, 179, 222–226

- yarn, 131, 133–136, 138–140, 142–144, 192, 193, 211, 232